Mine Water and the Environment (2006) 25: 86–92 © IMWA Springer-Verlag 2006

Technical Article

Summary of Deepwater Sediment/Pore Water Characterization for the Metal-laden Berkeley Pit Lake in Butte, Montana

Larry G. Twidwell[1], Christopher H. Gammons[2], Courtney A. Young[1], Richard B. Berg[3]

[1]Dept of Metallurgical and Materials Eng, Montana Tech, Butte MT 59701, USA; [2]Dept of Geological Eng, Montana Tech, Butte MT; [3]Montana Bureau of Mines and Geology, Butte MT; corresponding author's e-mail: LTwidwell@mtech.edu

Abstract. Unconsolidated sediment at the bottom of the Berkeley pit lake is a mixture of detrital silicate minerals derived from sloughing of the pit walls and secondary minerals precipitated out of the water column. The latter include gypsum and K-rich jarosite. The pore waters have a similar pH to the overlying lake waters (pH 3.1 to 3.4), and have similarly high concentrations of dissolved heavy metals, including Al, Cd, Cu, Mn, Ni, and Zn. Sediment cores show that the top meter of the sediment column is moderately oxidized (jarosite-stable). Petrography, chemical analysis and geochemical modelling all suggest a transformation of poorly crystalline ferric compounds such as schwertmannite and/or ferrihydrite near the sediment surface to jarosite with depth in the core. No evidence of bacterial sulfate reduction was found in this study, despite the presence of 0.3 to 0.4 wt % organic carbon in the pit lake sediment.

Key words: acid mine drainage; characterization; geochemistry; jarosite; pit lake; pore water; schwertmannite; sediment; solubility

Introduction

The general features of the historical formation and chemical characteristics of the Berkeley Pit lake have been presented in the companion paper by Gammons and Duaime (2006) and will not be repeated here. The main objective of the present study is to characterize the chemistry and mineralogy of solids and pore fluids in the uppermost meter of the pit lake sediment, and to form hypotheses as to the chemical or biological reactions that may or may not be occurring in this unique benthic environment. One of the key questions that we set out to answer was whether or not sulfate reduction was occurring in the pit lake sediment. If so, this would have important implications to possible in-situ bio-remediation of the acidic and metal-laden waters in the overlying water column. Details not given in the present summary paper regarding the sampling program, the methods used for chemical and mineralogical characterization of the sediment and sediment pore waters, as well as the complete tables of analytical results, are available in Twidwell et al. (2000).

Methods

Two sediment surface solid samples for preliminary characterization were retrieved on Nov. 1997 at 182 m (600 ft) and 213 m (700 ft) depths (location unspecified). A more detailed sampling including three core samples (Cores 1, 2, and 3) and one deep water sample (BPD-1) was conducted at a site near the maximum depth of the Berkeley Pit lake in April and May 1998. Sampling was conducted using a NISKEN vertical sampler for collecting deep water samples and a Benthos sediment core sampling device for the core and pore water samples. The location of the core-sampling site was Latitude 46° 01' 03.50", Longitude 112° 30' 41.00" at an approximate surface water/sediment depth of 220 m.

Each of the core samples was approximately 70-90 cm long and 10 cm in diameter. The Benthos sampling device allowed for solids and associated pore waters to be retrieved intact without contamination or disturbance during withdrawal from the sampling site. The sediment in all three cores had a pale yellow to pale-reddish brown color. These visual observations indicated early on that bacterial sulfate reduction was unlikely to have occurred, as this would have imparted a black or dark gray color to the solids. The sediment and pore waters were protected from oxidation by placing the core in a Type A BBL Bio-Bag (© BD Clinical Laboratory Solutions). Then the cores were transported to the Montana Tech Metallurgical Engineering laboratory and each was placed through an airtight seal into a glove box containing an argon atmosphere. The core-column was raised by a hydraulic lift to a desired height and the core was then sectioned into 2-10 cm core lengths for chemical characterization of both the solids and the pore water (Figure 1). The core slices contained from 17 to 48 wt% solids with the higher solids content present at the bottom of each core. The pore water was recovered from the individual slices by centrifuging. After measuring pH and electrical potential (E_H) of the centrifuged water, triplicate 20- mL aliquot pore fluid samples in each section were filtered

Figure 1. Photograph of sample sectioning for transferring to a storage vessel, using a deoxygenated glovebox

through a 0.45 µm surfactant free cellulose acetate (SFCA) filter disk and preserved with 1 ml high purity HNO_3 for chemical analysis. Split samples were diluted and preserved with HCl for determination of Fe(II) and total Fe by the 1,10-phenanthroline method. Digestion of the solids was performed utilizing U.S. EPA SW-846, Method 3052A (U.S. EPA 1995). The separated pore waters and solid digestates were analyzed for a suite of major and trace elements by SW-846, Method 6010A (U.S. EPA 1993) using an Inductively Coupled Plasma Emission Spectrometer (ICP-ES). All analytical data presented in subsequent tables are averages of triplicate analyses.

Results

Sediment Pore Water Compositions

Sediment pore water compositions for Core 1 are given in Tables 1 and 2, along with an analysis of the pit lake water immediately above the sediment-lake interface (BPD-1). Data for Cores 2 and 3 (not shown) showed very similar trends, and are omitted for lack of space. A comparison of the deep lake water and sediment pore water compositions shows that the upper pore waters had a lower concentration of Al, K, P, and As, and a higher concentration of Fe and S. With depth in the core, the concentrations of Fe decreased to values similar to the overlying lake waters, whereas concentrations of dissolved Cu increased. Concentrations of other solutes, including Ca, Cd, Mg, Mn, Na, Ni, Pb, Si, and Zn, were invariant with depth or showed inconsistent trends.

The pH of the sediment pore waters (measured at ambient temperature, 23-26°C) ranged from 3.1 to 3.4 (Table 2), and showed very little change with depth. The laboratory pH of water from the pit lake at a depth immediately above the core was 3.1, and the pH measurements of pore water from the other sediment cores were also in the range of 3.1 to 3.4. These results indicate a very strong pH buffering in the system, probably due to reactions involving aqueous Fe and SO_4^{2-}/HSO_4^-. A systematic trend of decreasing E_H with depth was documented for Core 1 (Table 2), as well as Cores 2 and 3 (data not shown).

Results of the Fe speciation analyses showed a trend of decreasing Fe(II)/Fe(III) ratio with depth, which is inconsistent with the E_H data. This problem most likely reflects partial oxidation of Fe(II) to Fe(III) prior to analysis. Therefore the Fe speciation data are suspect and are not reported here.

Characterization of solids

The chemical compositions of depth-sectioned solid samples from the three cores retrieved during the April

Table 1. Composition of deep pit lake water and Core 1 pore water (mg/L) relative to sample depth (cm); samples collected April 22, 1998

Sample slice, depth	Al	As	Ca	Cd	Cu	Fe	K	Mg	Mn	Na	Ni	P	Pb	S	Si	Zn
Deep Pit Lake Water																
BPD-1(avg)	293	0.89	477	2.4	191	1100	8.2	491	235	110	1.2	0.8	0.04	2825	54	646
Sediment pore water, Core 1																
0-5	185	0.03	454	2.5	197	2480	4.4	482	232	182	1.2	0.4	0.05	3432	50	621
5-10	154	0.17	442	2.5	196	2830	4.0	474	235	105	0.0	0.5	0.20	3454	49	613
10-15	129	0.22	428	2.4	186	2710	2.0	458	226	74	1.1	0.5	0.32	3358	48	588
15-20	126	0.12	429	2.4	187	2390	1.4	450	220	93	1.1	0.5	0.09	3091	50	586
20-25	145	0.10	431	2.4	247	2010	1.4	465	217	90	1.2	0.4	0.06	2966	53	601
25-35	187	0.13	431	2.3	347	1610	1.3	458	211	100	1.2	0.2	0.07	2794	61	599
35-45	217	0.16	441	2.2	381	1320	1.6	443	210	95	1.1	0.5	0.09	2631	66	603
55-60	225	0.07	439	2.3	410	1280	2.4	456	208	99	1.3	0.3	0.04	2680	65	601
60-65	228	0.11	441	2.3	420	1250	1.7	461	207	106	1.3	0.4	0.03	2729	66	598
65-69	222	0.20	436	2.2	409	1220	2.9	445	203	100	1.1	0.4	0.10	2637	70	590

Table 2. The pH, E_H and calculated iron speciation[1] of pore waters for Core 1

Measured parameters				Calculated by V-MINTEQ		
Depth, cm	E_H, mV[2]	pH[2]	Tot. Fe	$Fe^{(II)}$	$Fe^{(III)}$	$Fe^{(II)}/Fe^{(III)}$
0-5	562	3.1	2480	2430	50	49
5-10	532	3.1	2830	2811	19	148
10-15	510	3.2	2710	2702	7.5	360
15-20	478	3.3	2390	2388	2.0	1190
20-25	470	3.4	2010	2009	1.3	1540
25-35	492	3.3	1610	1608	2.2	731
35-45	489	3.3	1320	1318	1.6	824
55-60	487	3.3	1280	1279	1.4	913
65-69	488	3.3	1220	1219	1.4	870

[1]Fe concentrations in mg/L; [2]measured at ambient temperature, 23-26°C

22-23, 1997 sampling events are summarized in Tables 3 (Core 1) and 4 (Cores 2 and 3). The dominant elements in the solids were Si > Fe > Al > S > K. All other elements comprised less than 1% of the samples. There were general trends of decreasing Fe and S concentrations and decreasing Fe/K ratios with depth, which are discussed below. Total inorganic carbon (TIC) and total organic carbon (TOC) were measured on two samples from Core 2 and Core 3 (Table 4). Whereas TIC was below detection, TOC concentrations were in the range of 0.3 to 0.4 wt %.

Table 3. Composition (wt %) of Core 1 solids as a function of core depth (cm)

Depth	0-5	5-10	10-15	15-20	20-25	25-35	35-45	55-60	60-65	65-69
Al	6.1	6.2	6.3	5.3	5.9	8.1	7.3	5.2	5.3	6.6
As	0.10	0.10	0.12	0.14	0.07	0.15	0.07	0.06	0.07	0.07
Ca	0.6	0.7	0.7	0.5	0.7	0.7	0.5	0.4	0.4	0.5
Cu	0.25	0.24	0.29	0.29	0.31	0.43	0.51	0.52	0.62	0.69
Fe	15.4	11.7	12.0	10.0	7.4	10.0	7.2	6.8	6.5	6.0
K	1.57	1.57	1.60	1.57	1.75	1.76	1.38	1.05	1.06	1.21
Mg	0.79	0.77	0.86	0.47	0.55	0.79	0.69	0.37	0.54	0.73
Mn	0.08	0.07	0.08	0.07	0.06	0.06	0.07	0.07	0.07	0.08
Na	<0.1	<0.1	<0.1	0.14	0.20	0.64	<0.1	<0.1	2.18	<0.1
Pb	0.07	0.07	0.13	0.11	0.08	0.07	0.05	0.05	0.05	0.06
S	3.52	2.82	3.31	2.96	2.95	2.17	1.18	0.99	1.15	1.32
Si	13.0	14.9	16.0	17.4	20.3	20.3	20.3	19.0	17.5	19.0
Zn	0.16	0.14	0.23	0.15	0.13	0.14	0.17	0.15	0.18	0.21

DL=detection limit

Table 4. Composition (wt %) of Cores 2 and 3 solids as a function of core depth (cm)

	Core 2								**Core 3**		
Depth	0-2	2-4	4-6	6-8	8-10	18-20	45-47	67-72	0-5	45-50	75-80
Al	12.4	5.4	6.5	6.7	7.5	6.7	7.2	7.3	7.0	4.5	7.3
As	0.25	0.11	0.13	0.09	0.06	0.08	0.16	0.07	0.09	0.07	0.04
Ca	1.3	0.6	0.7	0.6	0.8	0.5	0.4	0.5	0.6	0.3	0.6
Cu	0.5	0.2	0.3	0.3	0.3	0.2	0.3	0.5	0.3	0.5	0.4
Fe	29.1	13.6	14.8	13.2	9.0	12.8	11.2	6.7	12.6	5.6	6.9
K	3.2	1.6	1.7	1.5	1.9	1.6	1.8	1.4	1.6	0.8	1.3
Mg	1.6	0.6	0.8	0.9	1.0	0.8	0.7	0.8	0.9	0.5	0.5
Mn	0.1	0.1	0.06	0.06	0.06	0.08	0.07	0.07	0.07	0.06	0.08
Na	<0.1	<0.1	<0.1	<0.1	<0.1	<0.1	0.46	<0.1	<0.1	<0.1	<0.1
Pb	0.15	0.05	0.07	0.07	0.04	0.08	0.13	0.05	0.10	0.06	0.03
S	6.7	2.9	3.8	2.8	1.9	2.4	3.0	1.2	2.8	1.0	0.6
Si	31.2	13.2	18.9	16.0	21.8	17.5	15.8	18.2	16.6	17.7	20.6
Zn	0.30	0.10	0.12	0.13	0.11	0.14	0.15	0.16	0.18	0.15	0.10
TIC[1]	<0.1										<0.1
TOC[2]	0.30										0.40

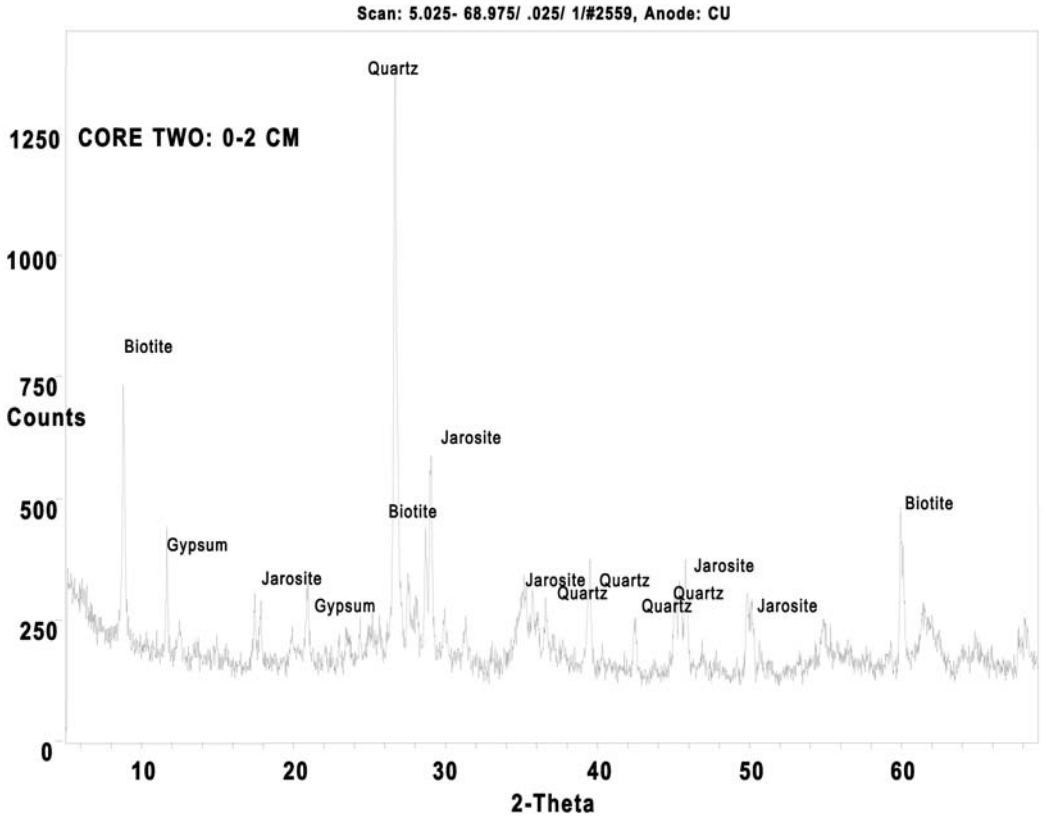

Figure 2. X-ray diffraction pattern for the sediment solid surface slice (0-2 cm) from core-2; the peaks labelled biotite are probably a mixture of biotite and muscovite.

X-ray diffraction (XRD) studies were conducted on 40% of the core segments. A typical pattern is presented in Figure 2. Crystalline phases identified in all of the samples included quartz, jarosite (perhaps a mixture of potassium and hydrogen jarosite), biotite (perhaps a mixture of muscovite and biotite), and gypsum. Samples were separated into two size fractions: > 325 mesh (> 44 µm) and < 325 mesh (< 44 µm). A comparison of the XRD patterns showed a higher abundance of jarosite in the < 325 mesh fraction. This agrees with scanning electron microscope (SEM) imagery, which revealed the majority of the jarosite grains to be less than 2 µm in diameter. In general, K-bearing jarosite was the most abundant secondary mineral identified by SEM, and formed fine coatings on detrital minerals such as mica, feldspar, and quartz. Jarosites were identified in all samples, irrespective of depth in the core.

Petrographic examination of impregnated thin sections of the sediment core slices was performed using a conventional polarizing microscope for roughly 20% of the samples. The mineralogy of all samples examined was similar; the only difference was in the relative proportion of the individual minerals. The thin section examinations agreed with the XRD and SEM analyses, and indicated a mixture of coarser-grained, detrital minerals (mainly quartz, altered feldspar, biotite, muscovite, with trace pyrite, zircon, apatite, hornblende, and epidote), and finer-grained secondary precipitates (mainly gypsum and jarosite). The pyrite grains that were identified were coarsely crystalline with pseudo-cubic morphology, indicating a primary (hydrothermal) vs. secondary (biogenic) origin.

Discussion

Geochemical Modelling

Geochemical modelling of sediment pore water was performed using the program Visual MINTEQ, version 2.32. This program is a recent adaptation of the original MINTEQ program by Allison et al. (1991) and can be downloaded at the following website: www.lwr.kth.se/English/OurSoftware/vminteq/. The MINTEQ database was supplemented with thermodynamic data for schwertmannite (Bigham et al. 1996). Because we were unable to obtain in situ measurements of the temperature of the sediment pore waters, the calculations were performed at 25°C, i.e., the same temperature at which the pore water pH and E_H were measured. Although the deep pit lake waters are cold (less than 8°C, Gammons and Duaime 2006), the surrounding fractured bedrock and groundwater are warm (> 20°C, Gammons et al.

2006). It is conceivable that the sediment-water interface at the bottom of the pit lake is also a type of thermocline, separating overlying cold lake water from warm pore water in the underlying sediment. Unfortunately, no data exist to further evaluate this possibility at this time.

To calculate the saturation indices of Fe(III) minerals, the Fe(II)/Fe(III) ratio of each water sample was manually adjusted until the E_H values calculated by V-MINTEQ agreed with the measured E_H values. As discussed by Nordstrom and Alpers (1999) and Nordstrom et al. (1979), it is possible to achieve excellent agreement between measured E_H values and Fe(II)/Fe(III) ratios determined separately by colorimetric measurement of acid mine waters when dissolved Fe concentrations are greater than 10^{-5} molal. All of the pore waters in this study contain much higher dissolved Fe concentrations (> 0.02 molal). The resultant speciation of Fe calculated by V-MINTEQ is summarized in Table 2.

Results of the V-MINTEQ modelling suggest that all of the pore fluids were near equilibrium saturation with gypsum (S.I. = -0.03 to +0.02), amorphous silica (S.I. = 0.00 to +0.15), and $AlOHSO_4$ (S.I. = -0.24 to +0.24). The latter phase has no mineral name, but is sometimes considered a proxy for poorly crystalline Al hydroxy-sulfate minerals that commonly form in acidic mine waters. No compounds of Cd, Cu, Mn, Pb, or Zn were found to be anywhere near saturation for any of the pore waters. The concentrations of these elements in the pore fluids were probably controlled by the abundance of source minerals that are dissolving along the exposed pit walls and sediment pile. At the low pH of the waters in question (3.1 to 3.4), none of these cationic metals should adsorb strongly onto secondary Fe compounds (Dzombak and Morel 1990). In contrast, both P and As (mainly present as orthophosphate and arsenate/arsenite, respectively) are known to adsorb strongly onto ferric precipitates in the pH range 3 to 4 (Dzombak and Morel 1990), and this helps to explain the lower concentrations of these solutes in the sediment pore waters relative to the overlying pit lake. It is also possible that some of the transition metals could co-precipitate with jarosite as a solid impurity. Lead has a particular affinity for jarosite, forming so-called plumbo-jarosite in Pb-rich environments (Dutrizac and Jambor 2000).

Results of saturation index (S.I.) calculations for selected Fe(III)-bearing mineral phases are summarized in Figure 3. In this figure, the S.I. values calculated by V-MINTEQ have been adjusted to one Fe atom per formula unit, so that a more equitable comparison can be made for the various ferric compounds. For

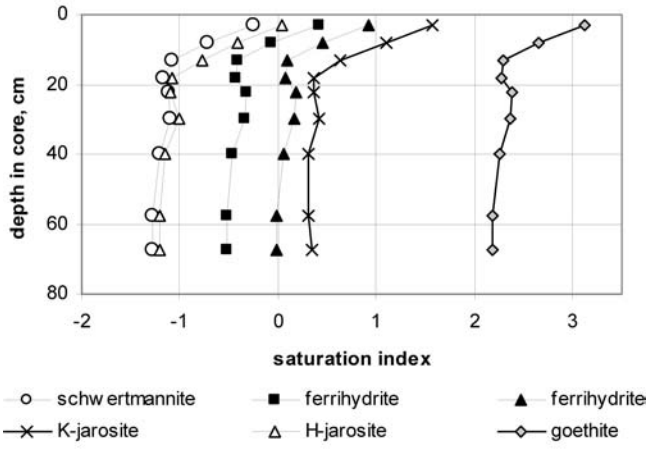

Figure 3. Saturation indices (S.I.) of selected Fe(III) solids in sediment pore water from Core 1. These data were generated using Visual MINTEQ. All S.I. values have been adjusted to one Fe atom per formula unit (see text).

example, the S.I. for jarosite, $KFe_3(SO_4)_2(OH)_6$, was divided by 3, since the mineral has 3 Fe atoms in its formula. The pore waters near the surface of the sediment pile were shown to be close to equilibrium saturation with schwertmannite and H-jarosite, but supersaturated with K-jarosite, goethite, and ferrihydrite. However, with depth in the core, the fluids become undersaturated with schwertmannite and freshly precipitated ferrihydrite, and very close to equilibrium with K-jarosite and "aged" ferrihydrite. These trends are believable, and are consistent with several lines of evidence presented earlier in this paper, as well as by previous workers, as outlined below.

Robins et al. (1997) and Pellicori et al. (2005) conducted geochemical modelling on two different sets of data from the Berkeley pit lake, and came to the independent conclusion that the shallow lake waters are saturated or super-saturated with schwertmannite. Furthermore, this phase has been positively identified by SEM as an abundant secondary coating on the surface of a submerged rope left in the pit lake for an extended period of time (see Gammons and Duaime 2006, Figure 5), and also by Newbrough and Gammons (2002) in bench-top studies of water-rock interaction of Berkeley pit water with pit wallrock. It is logical to assume that schwertmannite particles forming near the surface of the pit lake would descend by gravity through the water column to collect near the surface of the sediment pile.

Once buried, the thermodynamic calculations suggest that the schwertmannite should be dissolving (S.I. values become negative in Figure 3) at the same time as precipitation or recrystallization of aged

ferrihydrite and/or K-jarosite. The conversion of schwertmannite to K-jarosite can be written as follows:

$$3Fe_8O_8(SO_4)(OH)_6 + 6H_2O + 8K^+ + 13SO_4^{2-} + 18H^+ = 8KFe_3(SO_4)_2(OH)_6 \quad (1)$$

By the stoichiometry of reaction 1, the transformation of schwertmannite to jarosite should be accompanied by an increase in solution pH and a decrease in the K^+ concentration of the pore waters. These predicted trends agree with results summarized in Tables 1 and 2. Furthermore, the data in Tables 3 and 4 show that the Fe:K ratio of the solids in the sediment core decreased with depth. Since jarosite has the ideal formula of $KFe_3(SO_4)_2(OH)_6$, one would expect an Fe:K mole ratio of 3 if K-jarosite was the dominant Fe- and K-bearing mineral in the sediment. Whereas the Fe:K mole ratios in the solids are > 5 for the near-surface pore waters, this ratio drops to 3.4 to 3.7 for the sediment slices deepest in the core. Because schwertmannite contains no potassium, the higher Fe:K ratios near the surface are consistent with the presence of this phase, or perhaps ferrihydrite. Obviously, this discussion is complicated by the fact that there are other Fe-bearing minerals (such as biotite and pyrite) and K-bearing minerals (such as biotite and muscovite) present in the sediments. However, the overall trends based on the chemistry of the pore waters and co-existing solids support the hypothesis based on V-MINTEQ modelling that there is a gradual conversion of schwertmannite to jarosite with depth in the sediment pile.

A major question that remains partly unanswered is whether or not there are microbial redox reactions occurring in the pit lake sediment. The TOC analyses from Core 3 (Table 4) show that a fair amount of organic carbon is present (0.3 to 0.4%), although these concentrations are much lower than what would be expected for a healthy, biologically-productive lake. The oxidized nature of the core samples – based on visual observation (color), microscopic examination, and the measured and calculated E_H values – precludes the existence of any significant bacterial sulfate reduction. More than likely, the low pH and extremely high heavy metal concentration of the pore fluids creates too harsh of an environment for sulfate-reducing bacteria. However, it is possible that some bacterial *iron reduction* is occurring in the sediment column. This would be consistent with the trends of lower E_H and higher dissolved Fe(II)/Fe(III) ratio (based on the calculated redox speciation of iron) with depth in the core. If so, then it is quite possible that the presumed dissolution of schwertmannite in the upper section of the core could have been enhanced by microbial reduction (e.g. see Regenspurg et al. 2002). This would also explain the dramatic increase in total Fe and Fe(II) concentrations in the top 20-30 cm of the sediment column. Additional work focusing on the microbiology of the pit lake and sediment pile is needed to confirm or refute these hypotheses.

Conclusions

This paper documents the chemical composition of solids and coexisting pore waters in the upper meter of sediment collected at the bottom of the Berkeley pit lake. Overall, the chemistry of the pore waters has a similar pH and metal content as the overlying lake waters. The pit lake sediments are not sulfidic, but do show a general trend of lower redox potential with depth. Although the observed mineralogy of the sediment pile did not change in an obvious way with depth, thermodynamic calculations suggest that schwertmannite may be dissolving near the top of the sediment pile, and then re-precipitating as K-jarosite deeper in the pile. Further work is needed to confirm whether these changes are indeed occurring, and whether they are mediated by bacteria or are the result of essentially abiotic processes.

Acknowledgements

We thank the U.S. Environmental Protection Agency Mine Waste Technology Program for their funding of this study (Interagency Agreement No: DW89938513-01-0). We also thank Jim Jonas, Bill Chatham, and the MBMG samplers who assisted in our study. The paper was improved by the comments of Charles Cravotta and an anonymous reviewer.

References

Allison JD, Brown DS, Novo-Gradak KJ (1991) MINTEQA2/PRODEAFA2, a geochemical assessment model for environmental systems. US Environmental Protection Agency, EPA/600/3-91/021

Bigham JM, Schwertmann U, Traina SJ, Winland RL,Wolf M (1996) Schwertmannite and the chemical modeling of iron in acid sulfate waters. Geochim Cosmochim Acta 60: 2111-2121

Dutrizak JE, Jambor JL (2000) Jarosites and their application in hydrometallurgy. Mineralogical Soc of America, Reviews in Mineralogy and Geochemistry, 40: 405-452

Dzombak DA, Morel FMM (1990) Surface Complexation Modeling: Hydrous Ferric Oxide. Wiley-Interscience, New York, USA, 416 pp

Gammons CH, Duaime TE (2006) Long term changes in the limnology and geochemistry of the

Berkeley pit lake, Butte, Montana, Mine Water Environ 25(2): 76-85

Gammons CH, Metesh JJ and Snyder DM (2006) A survey of the geochemistry of flooded mine shaft water in Butte, Montana. Mine Water Environ 25(2): 100-107

Newbrough P, Gammons CH (2002) Experimental investigation of water-rock interaction and acid mine drainage at Butte, Montana. Environ Geol 41: 705-719

Nordstrom DK, Alpers CN (1999) Geochemistry of acid mine waters. Soc of Economic Geologists, Reviews in Economic Geology 6A: 133-160

Nordstrom DK, Jenne EA, Ball JW (1979) Redox equilibria of iron in acid mine waters. In Jenne EA (ed), Chemical Modeling in Aqueous Systems, Am Chem Soc Symp Series 93: 51-80

Pellicori DA, Gammons CH, Poulson SR (2005) Geochemistry and stable isotope composition of the Berkeley pit lake and surrounding mine waters, Butte, Montana. Applied Geochem 20: 2116-2137

Regenspurg S, Gößber A, Peiffer S, Küsel K (2002) Potential remobilization of toxic anions during reduction of arsenated and chromated schwertmannite by the dissimilatory Fe(III)-reducing bacterium Acidiphilium Cryptum JF-5. Water Air Soil Poll, Focus 2: 57-67

Robins RG, Berg RB, Dysinger DK, Duaime TE, Metesh JJ, Diebold FE, Twidwell LG, Mitman GG, Chatham WH, Huang HH, Young CA (1997) Chemical, physical and biological interaction at the Berkeley Pit, Butte, Montana. Proc, Tailings and Mine Waste '97, Balkeema Press, Rotterdam, p 521-541

Twidwell L, Young C, Berg R (2000) Final Report-deep water characterization and interactions. Mine Waste Technology Program, Activity IV, Project 9; MWTP-133, 75 pp

U.S. EPA (1993) Methods for the Determination of Inorganic Substances in Environmental Samples. EPA/600/R-93/100, Washington DC, USA

U.S. EPA (1995) Test Methods for Evaluating Solid Waste-Physical/Chemical Methods. EPA/SW-846-IIB, Washington DC, USA

Submitted April 12, 2006; accepted May 10, 2006